www.czasopisma.pan.pl PAN POLSKA AKADEMIA NAUK www.journals.pan.pl

PAN ARCHIVES OF ACOUSTICS
Vol. **44**, No. 2, pp. 309–320 (2019)
DOI: 10.24425/aoa.2019.128494

Vibration Analysis of a Carbon Nanotube Reinforced Uniform and Tapered Composite Beams

Ananda BABU ARUMUGAM[(1)], Vasudevan RAJAMOHAN[(2)], Naresh BANDARU[(3)]
Edwin SUDHAGAR P.[(4)], Surajkumar G. KUMBHAR[(5)]

[(1)] *Department of Mechanical Engineering, SET*
Sharda University
Greater Noida, India, 201 306

[(2)] *Center for Innovative Manufacturing Research*
Vellore Institute of Technology
Vellore, India

[(3)] *Department of Mechanical Engineering*
Brilliant Institute of Engineering and Technology
Hyderabad, Telangana, 501 505

[(4)] *School of Mechanical Engineering*
Vellore Institute of Technology
Vellore, India
Corresponding Author e-mail: edwinsudhagar.p@vit.ac.in

[(5)] *Department of Automobile Engineering*
Rajarambapu Institute of Technology
Sakhrale, Sangli, Maharashtra, India, 415 414

(*received March 7, 2018; accepted December 8, 2018*)

In this study, free and forced vibration responses of carbon nanotube reinforced uniform and tapered composite beams are investigated. The governing differential equations of motion of a carbon nanotube (CNT) reinforced uniform and tapered composite beams are presented in finite element formulation. The validity of the developed formulation is demonstrated by comparing the natural frequencies evaluated using present FEM with those of available in literature. Various parametric studies are also performed to investigate the effect of aspect ratio, percentage of CNT content, ply orientation, and boundary conditions on natural frequencies and mode shapes of a CNT reinforced composite beam. It was observed that the addition of carbon nanotube in fiber reinforced polymer composite (FRP) beam enhances the stiffness of the structure which consequently increases the natural frequencies and alters the mode shapes.

Keywords: carbon nanotubes; uniform and tapered composite beams; finite element formulation; natural frequency.

1. Introduction

Fiber-reinforced polymer composites (FRP) are extensively being used across a broad spectrum of engineering applications, including aerospace structures, sports equipment and wind turbines due to their strong and lightweight characteristics which leads to an alternative over traditional building materials (Soutis, 2005). However, the applications are often limited due to their low damping factor resulting from poor viscoelastic nature of fibers and poor damping at the FRP interface. Various methods have been suggested to improve the damping characteristics of composite structures such as addition of high damping polymer layers in prepreg lay-up (Saravanos, Pereira, 1992) and use of hybrid rubber particle reinforced composites (Moser, Lumassegger, 1988). Conversely, damping properties are enhanced at a cost of reduced mechanical properties of the composites.

Since the discovery of carbon nanotubes (CNTs) by Iijima (1999) and the realization of their unique physical properties (including mechanical, thermal, and electrical properties), significant attention has been focused by many investigators to fabricate advanced CNT composite materials that exhibit one or more of these properties to improve the damping properties. As the specific stiffness of CNTs is very high ($E \sim 1$–2 TPa), the stiffness of the reinforced structure could be increased significantly which leads to increase in natural frequencies of the structure. Hence, the reinforcement of CNTs in composite structures increases the natural frequencies as well as damping.

Many studies (Andrews, Wiesenberger, 2004; Bakshi *et al.*, 2009) have been reported on characterization of carbon nanotube-reinforced composites (CNTRCs). Several investigations (Ruoff *et al.*, 2003; Shi *et al.*, 2004) have also shown that the addition of small amounts of carbon nanotube in FRP composites can considerably improve their mechanical and electrical properties. It was reported (Fidelus *et al.*, 2005; Tan *et al.*, 2007) that an increase of interface adhesion between carbon nanotubes and polymer matrix may improve the composite behaviour at the large strain significantly. Also, it was mentioned (Ko, 2004) that the aspect ratio of the nanotube and the type of interface between CNT and the polymer matrix play a vital role in tailoring the strength of a CNT reinforced composite. The effect of volume fraction and L/D ratio of CNTs in a beam has been investigated (Deepak *et al.*, 2012) experimentally on the natural frequency of a CNT reinforced composite beam. In concern with the importance of alignment of CNT in polymer, it was experimentally shown (Thostenson, Chou, 2002) that the elastic modulus of the uniformly aligned CNT could be enhanced almost five times comparing to that of randomly oriented composite. The mechanical and damping properties of the CNTRCs are assessed (Savvas *et al.*, 2012) on the basis of sensitivity analysis with respect to various weight fractions and values of interfacial shear strength (ISS). The dynamic mechanical analysis confirmed that addition of CNTs into composites increases its damping ratio (approximately by 0.3). It was also shown (Khan *et al.*, 2011) that both the dynamic loss modulus and loss factor of the nanocomposites could be increased with the addition of CNTs. A finite element model of the CNT/epoxy composite interface was developed (Dai, Liao, 2009) for different strains and orientations of CNT within the matrix. It was also shown (Lin, Lu, 2010) that the damping effect of CNTs embedded matrix composites offers the potential for designing a passive damping mechanism into functional composite materials. The composites reinforced with CNTs have been also demonstrated (Gibson *et al.*, 2007) for enhanced damping characteristics compared to an identical material without the addition of CNTs.

Recently, experimental investigation (Jakkamputi, Rajamohan, 2017) of dynamic characteristics of glass fiber-reinforced epoxy composite (GFRP) beam with and without CNT reveals the enhancement in the bending stiffness of hybrid composite (CNTGFRP) comparing to that of neat GFRP. Additionally, substantial decrease in fundamental natural frequency of CNTGFRP composite beam and increase in the damping ratio have been shown owing to occurrence of stick slip mechanism and transformation of interfacial bond between CNT and epoxy at elevated temperature.

Many investigations (Ramaratnam, Jalili, 2006) have also shown that the CNTs tends to stick to each other and constructing uniformly dispersed CNT composites was difficult which causes inadequate enhancement in the expected elastic moduli of CNT composites. Damping properties of CNT reinforced resin based composite structures have been studied (de Borbon *et al.*, 2014) in which a smaller aspect ratio in multi-walled non-functionalized nanotubes were found to be the most effective to improve the damping properties of simple as well as sandwich beams. Furthermore, many pertinent works were presented to investigate the dynamic characteristic of uniform and tapered composite structures without CNT reinforcement. A review of recent developments has been presented (He *et al.*, 2000) where an analysis of tapered laminated composite structures emphases on inter-laminar stress analysis and delamination analysis. A finite element model with nodal degrees of freedom which can satisfy all the forced and natural boundary conditions of a Timoshenko beam was presented first time by Thomas and Abbas (1978). Also, Cleghorn and Tabarrok (1997) demonstrated a finite element model for free vibration of linearly-tapered Timoshenko beams. The finite element formulation was developed (El-Maksoud Abd, 2000) for uniform and variable thickness composite beams. Various parametric studies were also performed to demonstrate the effect of different boundary conditions, fiber orientation and taper angle on the natural frequencies and buckling loads on the beams. The governing differential equations of motions of a tapered composite beam were derived (Zabihollah, Genesan, 2007) using conventional finite element formulation. Additionally, some key studies explored the effect of taper angle, types of taper, boundary conditions, laminate configuration and geometric parameters on the undamped natural frequencies.

Though several studies have been focused on dynamic characterization of uniform and tapered composite structures, a numerical approach to study the effect of CNT reinforcement on the dynamic properties of fiber reinforced polymer (FRP) composites has not been made. In the present study, the free vibration responses of uniform and tapered composite beams reinforced with CNTs are investigated. The governing dif-

ferential equations of motion of a FRP in both uniform and tapered composite beams without and with CNTs reinforcement are developed in the finite element formulation. The validity of the developed finite element formulation is demonstrated by comparing the results in terms of natural frequencies with those of available literature (Qu *et al.*, 2013). The natural frequencies of a composite beam without and with CNTs are also compared. Various parametric studies are also performed to investigate the effect of percentage content of CNTs, aspect ratio, ply orientation, mode shapes, and boundary conditions on the free vibration characteristics of CNT fiber reinforced polymer composite tapered beam.

2. Mathematical modelling of tapered composite beams without and with CNT reinforcement

Uniform and tapered composite beams made of orthotropic layers reinforced with CNTs are considered for the development of mathematical modelling. The CNTs are considered to be reinforced with resin which is further reinforced with the fiber to form a CNTs reinforced polymer fiber composite beam (CNTRPF). The CNT reinforced composite beam is considered to be thin and Kirchhoff's hypothesis in conjunction with the classical laminated plate theory is employed to model the composite layers.

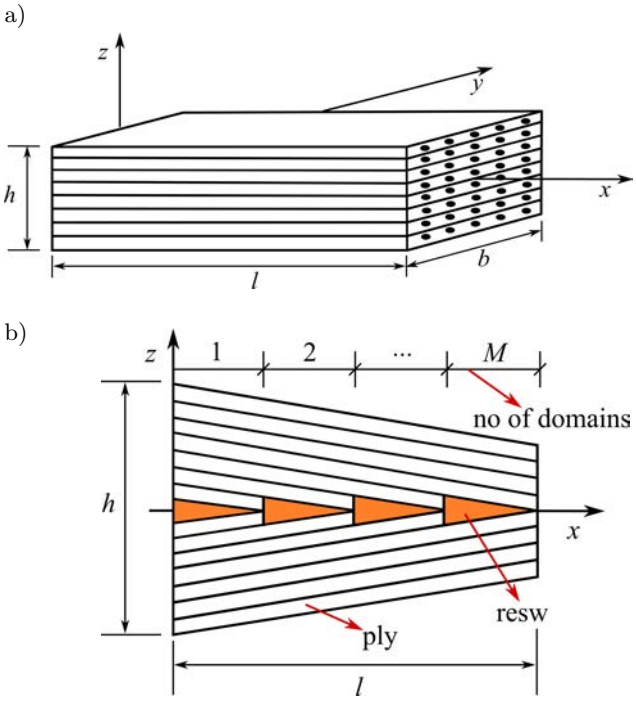

Fig. 1. Representation of a CNT reinforced: a) uniform, b) tapered composite beam.

The thickness h of the beam is considered to be very small compared to the length l and the width b of the beam. Therefore, shear strain and rotary inertia effects are neglected. The transverse deflection w is considered to be uniform throughout the cross section. Furthermore, the continuum mechanics modelling approach is implemented to represent the reinforcement of CNTs in fiber reinforced polymer composite beam.

2.1. Formulation of energy equation of a tapered composite beam with and without CNT reinforcement

The relationship between the stress and strain $(\sigma - \varepsilon)$ of a tapered composite beam along the global axes x, y and z is derived by transforming the stress and strain (σ'' and ε'') obtained along the fiber axes x'' and y'' into the oblique plane (x' and y' axes) by rotating the ply about an orientation angle θ about z'' axis and then by rotating about the taper angle α about y axis, as presented in Fig. 2, such that:

$$\{\sigma'\} = [T_{\sigma\theta}]\{Q''\}[T_{\sigma\theta}]^{\mathrm{T}}\{\varepsilon'\}, \tag{1}$$

$$\{\sigma\} = [\overline{Q}_{ij}]\{\varepsilon\}, \tag{2}$$

where

$$\left[\overline{Q}_{ij}\right] = [T_{\sigma\alpha}][T_{\sigma\theta}]\{Q''\}[T_{\sigma\theta}]^{\mathrm{T}}[T_{\sigma\alpha}]^{\mathrm{T}},$$

$$[T_{\sigma\theta}] = \begin{bmatrix} \cos^2\theta & \sin^2\theta & -2\cos\theta\sin\theta \\ \sin^2\theta & \cos^2\theta & 2\cos\theta\sin\theta \\ \cos\theta\sin\theta & -\cos\theta\sin\theta & \cos^2\theta - \sin^2\theta \end{bmatrix}$$

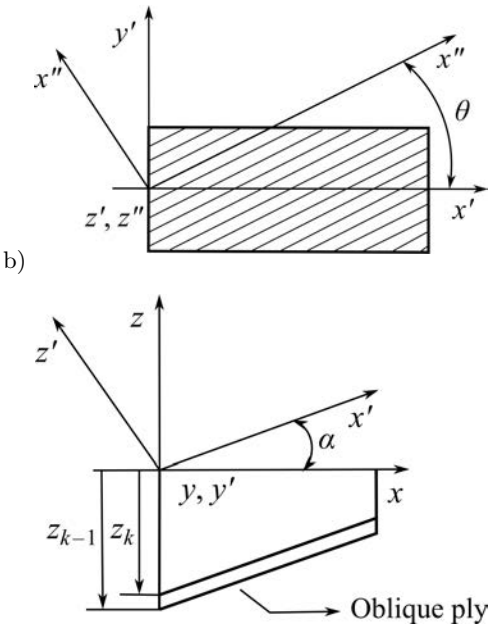

Fig. 2. a) Transforming (x'', y'', z'') coordinates to (x', y', z') coordinates, b) transforming (x', y', z') coordinates to (x, y, z) coordinates.

is the stress transformation matrix from (x'', y'', z'') coordinates to (x', y', z') coordinates and

$$[T_{\sigma\alpha}] = \begin{bmatrix} \cos^2\alpha & 0 & 0 \\ 0 & 1 & 0 \\ 0 & 0 & \cos\alpha \end{bmatrix}$$

is the stress transformation matrix from (x', y', z') coordinates to (x, y, z) coordinates.

Now, the potential energy of the CNT reinforced tapered composite can be represented as:

$$U^{\mathrm{CNT}} = \frac{1}{2}\int_0^l D_{11}^{\mathrm{CNT}} b\left(\frac{\partial^2 w}{\partial x^2}\right)^2 \mathrm{d}x, \tag{3}$$

where

$$D_{11}^{\mathrm{CNT}} = \sum_{k=1}^{N-M} \overline{Q}_{11}^{\mathrm{CNT}}\left(z_k^3 - z_{k-1}^3\right) + \sum_{k=N+M+1}^{2N} \overline{Q}_{11}^{\mathrm{CNT}}\left(z_k^3 - z_{k-1}^3\right) - 2\overline{Q}_r^{\mathrm{CNT}} z_{N-M}^3,$$

and

$$z_k = x\tan\alpha + h(k-N), \qquad h = \frac{t}{\cos\alpha},$$
$$\tan\alpha = \frac{(N-R)h}{l},$$

z_k is the thickness of each ply with taper angle; N is half layers at the left end of the tapered beam; R is half layers at the right end of tapered beam; h is the height of the tapered beam; t is the thickness of the each ply; l is the length of the beam and α is the taper angle.

The reduced stiffness matrix coefficient for a tapered composite beam with CNT reinforced ($\overline{Q}_{11}^{\mathrm{CNT}}$) can be expressed as:

$$\overline{Q}_{11}^{\mathrm{CNT}} = Q_{11}^{\mathrm{CNT}} c^4 + Q_{22}^{\mathrm{CNT}} s^4 + 2\left(Q_{12}^{\mathrm{CNT}} + 2Q_{66}^{\mathrm{CNT}}\right) s^2 c^2, \tag{4}$$

where

$$Q_{11}^{\mathrm{CNT}} = \frac{E_1^{\mathrm{CNT}}}{1 - v_{21}v_{12}}, \qquad Q_{12}^{\mathrm{CNT}} = \frac{v_{12}E_2^{\mathrm{CNT}}}{1 - v_{21}v_{12}},$$
$$Q_{22}^{\mathrm{CNT}} = \frac{E_2^{\mathrm{CNT}}}{1 - v_{21}v_{12}}, \qquad Q_{66}^{\mathrm{CNT}} = G_{12},$$
$$c = \cos\theta, \qquad s = \sin\theta.$$

The Young's modulus of each composite lamina with CNT in longitudinal direction, E_1^{CNT}, is given as (Ko, 2004):

$$E_1^{\mathrm{CNT}} = \left\{\left(\frac{3}{8}\right)\frac{1 + 2(L_{cnt}/D_{cnt})\eta_{L_1}v_{cnt}}{1 - \eta_{L_1}v_{cnt}} + \left(\frac{5}{8}\right)\frac{1 + 2\eta_{T_1}v_{cnt}}{1 - \eta_{T_1}v_{cnt}}\right\} E_{11}, \tag{5}$$

where $E_{11} = E_{fL}v_f + E_m v_m$, and E_m, E_{fL} are Young's modulus of matrix and fiber along the longitudinal direction; L_{cnt} and D_{cnt} are the length and diameter of the CNT, respectively; v_f, v_m, v_{cnt} are volume fraction of fiber, matrix and CNT respectively, and η_L, η_T and D_{cnt} are calculated as

$$\eta_{L_1} = \left\{\frac{(E_{cnt}/E_{11}) - 1}{(E_{cnt}/E_{11}) + 2(L_{cnt}/D_{cnt})}\right\},$$
$$\eta_{T_1} = \left\{\frac{(E_{cnt}/E_{11}) - 1}{(E_{cnt}/E_{11}) + 2}\right\},$$
$$D_{cnt} = \frac{\sqrt{3}}{\pi} d_{cc}\sqrt{n^2 + m^2 + nm},$$
$$\alpha = \frac{\pi}{3} - \cos^{-1}\left\{\frac{2m + n}{2\sqrt{n^2 + m^2 + nm}}\right\}.$$

The Young's modulus of each composite lamina with CNT in transverse direction, E_2^{CNT}, can be expressed as:

$$E_2^{\mathrm{CNT}} = \left\{\left(\frac{3}{8}\right)\frac{1 + 2(L_{cnt}/D_{cnt})\eta_{L_2}v_{cnt}}{1 - \eta_{L_2}v_{cnt}} + \left(\frac{5}{8}\right)\frac{1 + 2\eta_{T_2}v_{cnt}}{1 - \eta_{T_2}v_{cnt}}\right\} E_{22}, \tag{6}$$

where

$$E_{22} = \frac{1}{\frac{v_f}{E_{fT}} + \frac{v_m}{E_m}},$$
$$\eta_{L_2} = \left\{\frac{(E_{cnt}/E_{22}) - 1}{(E_{cnt}/E_{22}) + 2(L_{cnt}/D_{cnt})}\right\},$$
$$\eta_{T_2} = \left\{\frac{(E_{cnt}/E_{22}) - 1}{(E_{cnt}/E_{22}) + 2}\right\},$$

where E_{fT} is Young's modulus of fiber along the transverse direction and (n, m) is the chiral vector, α is the chiral angle of the nanotube in radian (right-hand convention), and $d_{cc} = 1.42 \cdot 10^{-10}$ m is the carbon-carbon bond length.

The kinetic energy of the CNT reinforced tapered composite beam can be expressed as:

$$T = \frac{1}{2}\int_0^l \rho A(x)\left(\frac{\partial w}{\partial t}\right)^2 \mathrm{d}x, \tag{7}$$

where $A(x)$ is varying area cross section of tapered composite beam, and $\rho = \rho^c$ – the density of the composite beam without CNTs which is expressed as:

$$\rho^c = \rho_f v_f + \rho_m v_m, \tag{8}$$

$\rho = \rho^{\mathrm{CNT}}$ – the density of the composite beam with CNTs which is expressed as:

$$\rho^{\mathrm{CNT}} = \rho_f v_f + \rho_{cnt} v_{cnt} + \rho_m v_m, \tag{9}$$

ρ_f, ρ_{cnt}, ρ_m are the density of fiber, CNT and matrix, respectively and v_f, v_{cnt}, v_m are the volume fraction of fiber, CNT and matrix, respectively.

2.2. Finite element formulation

The finite element model is developed by considering a standard beam element of length l_e with two end nodes and two degrees of freedom (DOF) at each node where DOFs are transverse direction (w) and rotational direction (θ), respectively. The transverse displacement is expressed in terms of nodal displacements and finite element shape functions as,

$$w(x,t) = N_w(x)\{d(t)\}, \tag{10}$$

where displacement vector, $d(t) = \{w_1, \theta_1, w_2, \theta_2\}$, and $N_w(x)$ is the composite beam shape functions which are expressed as:

$$N_1(x) = \frac{1}{4}\left(2 - 3\left(\frac{x}{l_e}\right) + \left(\frac{x}{l_e}\right)^3\right),$$

$$N_2(x) = \frac{1}{4}\left(1 - \frac{x}{l_e} - \left(\frac{x}{l_e}\right)^2 + \left(\frac{x}{l_e}\right)^3\right),$$

$$N_3(x) = \frac{1}{4}\left(2 + 3\left(\frac{x}{l_e}\right) - \left(\frac{x}{l_e}\right)^3\right),$$

$$N_4(x) = \frac{1}{4}\left(1 - \frac{x}{l_e} + \left(\frac{x}{l_e}\right)^2 + \left(\frac{x}{l_e}\right)^3\right).$$

The governing equations of motion of tapered composite beam with and without CNTs reinforcement are formulated using the Lagrange's method. The general Lagrange's equation can be expressed as:

$$\frac{\mathrm{d}}{\mathrm{d}t}\left(\frac{\partial T}{\partial \dot{q}_i}\right) - \frac{\partial T}{\partial \dot{q}_i} + \frac{\partial U}{\partial \dot{q}_i} = Q_i, \qquad i = 1, \ldots, n, \tag{11}$$

where n is the total DOF of the system considered for formulation of equation, Q_i is the generalized force corresponding to the i-th DOF of the system. By substituting the developed strain energy and kinetic energy equations for tapered (Eqs (3) and (7)) composite beams in the Lagrange's equation, an expression for governing equations of motion is obtained in the finite element form as:

$$[m^e]\{\ddot{d}\} + [k^e]\{d\} = \{f^e\}, \tag{12}$$

where $[m^e]$ is element mass matrix, $[k^e]$ is element stiffness matrix, and $\{f^e\}$ is the element force vector. Assembling all the element mass matrix, stiffness matrix and force vector, the global mass matrix, stiffness matrix and force vector can be evaluated and the global governing equations of motion is expressed as:

$$[M]\{\ddot{d}\} + [K]\{d\} = \{F\}. \tag{13}$$

2.3. Validation of the developed finite element formulation

The validity of the developed finite element formulation is demonstrated by comparing the natural frequencies evaluated using the present FEM with those available in literature (Qu *et al.*, 2013). The simulation is performed with the material and geometrical properties considered in (Qu *et al.*, 2013) such that:

$$E_1 = 144.80 \cdot 10^9 \text{ Pa}, \qquad E_2 = 9.65 \cdot 10^9 \text{ Pa},$$

$$G_{12} = 4.14 \cdot 10^9 \text{ Pa}, \qquad v_{12} = 0.3,$$

$$\rho = 1389.23 \text{ kg/m}^3, \qquad l = 0.762 \text{ m},$$

$$b = 0.00635 \text{ m}, \qquad h = 0.00635 \text{ m}.$$

Moreover, the bending stiffness co-efficient (D_{11}) is evaluated for the given material and geometric properties and substituted in the analytical solution available in (Rao, 2011) is presented as

$$\omega_n = (\beta_1 l)^2 \sqrt{\frac{bD_{11}}{\rho A l^4}}, \tag{14}$$

where $(\beta_1 l)$ are constants to be considered according to the boundary conditions.

The natural frequencies of a composite beam without CNTs are evaluated under simply supported end conditions with lay-up configuration of $[0°/0°]_s$ and the results are compared with those available in (Qu *et al.*, 2013) and the analytical solution available in (Rao, 2011) and presented in Table 1. Very good agreement observed among the result shows the effectiveness of the present FEM and extracting the bending stiffness co-efficient (D_{11}) and substitution in Eq. (14).

Table 1. Comparison of natural frequencies of a uniform composite beam without CNT reinforcement evaluated using the present FEM with (Qu *et al.*, 2013) and (Rao, 2011).

Mode No.	Present FEM	Qu *et al.* (2013)	Rao, (2011)	% error between present FEM and Qu *et al.* (2013)	% error between present FEM and Rao (2011)
1	50.78	50.77	51	0.019	0.43
2	203.12	203.11	203	0.004	0.05
3	457.02	456.91	454	0.020	0.66
4	812.49	812.29	804	0.020	1.04

Table 2. Comparison of natural frequencies of a uniform composite beam with CNT reinforcement evaluated using the present FEM with (Qu *et al.*, 2013).

Mode No.	C-F end conditions		S-S end conditions		C-C end conditions	
	Present FEM	Qu *et al.* (2013)	Present FEM	Qu *et al.* (2013)	Present FEM	Qu *et al.* (2013)
1	30.34	30.33	85.16	85.15	193.04	193.03
2	190.12	190.10	340.63	340.61	532.13	532.10
3	532.34	532.31	766.42	766.37	1043.20	1043.12
4	1043.20	1043.11	1362.50	1362.44	1724.50	1724.34

Table 3. Comparison of natural frequencies of a tapered composite beam with CNT reinforcement evaluated using the present FEM with (Qu *et al.*, 2013).

Mode No.	C-F end conditions		S-S end conditions		C-C end conditions	
	Present FEM	Qu *et al.* (2013)	Present FEM	Qu *et al.* (2013)	Present FEM	Qu *et al.* (2013)
1	38.57	36.75	75.97	76.68	176.57	173.82
2	187.97	171.19	308.58	306.72	484.77	479.15
3	489.19	479.34	692.11	690.11	937.10	939.33
4	932.55	939.32	1258.60	1226.88	1588.60	1552.00

The validity of the present FEM for evaluating the dynamic properties of a uniform composite beam with CNT reinforcement is investigated by comparing the natural frequencies of CNTs reinforced uniform composite beam with those evaluated using (Qu *et al.*, 2013). The various geometrical and material properties considered for the simulation are (Ko, 2004):

$$E_{fL} = 30.08 \cdot 10^9 \text{ Pa}, \quad E_{fT} = 6.78 \cdot 10^9 \text{ Pa},$$
$$E^m = 3.45 \cdot 10^9 \text{ Pa}, \quad G_{12} = 3.01 \cdot 10^9 \text{ Pa},$$
$$v_f = 0.256, \quad v_m = 0.3,$$
$$\rho_f = 1745 \text{ kg/m}^3, \quad \rho_m = 1200 \text{ kg/m}^3,$$
$$l = 0.3 \text{ m}, \quad b = 0.03 \text{ m},$$
$$h = 0.00315 \text{ m}, \quad \rho_{cnt} = 1300 \text{ kg/m}^3,$$
$$v_{cnt} = 0.01, \quad L_{cnt}/D_{cnt} = 50,$$
$$E_{cnt} = 1200 \cdot 10^9 \text{ Pa}.$$

The natural frequencies are evaluated under various boundary conditions including clamped-free (C-F), simply supported (S-S) at both ends and clamped-clamped (C-C) at both ends with the lay-up configuration of $[0°/90°]_{8s}$ and the results are also compared with the analytical solution available in (Qu *et al.*, 2013). The results are presented in Table 2. As it can be seen a decent agreement exists among the results evaluated using the present FEM and analytical solution.

The various geometrical and material properties of composite lamina and CNT considered for the simulation are (Ko, 2004):

$$E_{fL} = 30.08 \cdot 10^9 \text{ Pa}, \quad E_{fT} = 6.78 \cdot 10^9 \text{ Pa},$$
$$E^m = 3.45 \cdot 10^9 \text{ Pa}, \quad G_{12} = 3.01 \cdot 10^9 \text{ Pa},$$
$$v_f = 0.256, \quad v_m = 0.3,$$
$$\rho_f = 1745 \text{ kg/m}^3, \quad \rho_l = 1200 \text{ kg/m}^3,$$
$$l = 0.3 \text{ m}, \quad b = 0.03 \text{ m},$$
$$h = 0.00315 \text{ m}, \quad \alpha = 0.00266°,$$
$$\rho_{cnt} = 1300 \text{ kg/m}^3, \quad v_{cnt} = 0.01,$$
$$L_{cnt}/D_{cnt} = 50, \quad E_{cnt} = 1200 \cdot 10^9 \text{ Pa}.$$

The stacking sequence of the tapered composite beam at thick and thin sections are considered as $[0°/90°]_{8s}$ and $[0°/90°]_{4s}$ respectively. The thickness of each ply is 0.2 mm. Simulation is performed under two different boundary conditions including clamped-free (C-F) and simply supported (S-S) end conditions along both ends of the beam and the results are presented in Table 3 along with natural frequencies evaluated using the analytical solution available in (Qu *et al.*, 2013). A very good agreement can be observed among the results evaluated using the present FEM and available literature.

3. Results and discussions

Generally the CNT is used as filler in the polymer reinforced composite structures in order to improve the stiffness and damping of the structure. In this study, 0.01 to 0.05 volume fraction range of CNT is used in the glass reinforced polymer composites in order to get sufficient stiffness and damping as a structure. This range of volume fraction is achieved by using 0.015 to 0.06 of mass fraction of total composite. As 15 to 60 g of CNT is used for 1000 g of GRP composite structure and the production of CNT by CVD method with less cost, the cost of the CNT reinforced composite beam is significantly lower and it provides adequate mechanical properties. The free vibration responses of a CNT

reinforced composite beam are influenced by various properties including the volume fraction of CNT, aspect ratio of CNT, ply orientation and boundary conditions. Various parametric studies are performed to investigate the effect of those properties on natural frequencies and mode shapes of the uniform and tapered composite beams. The simulation is performed by considering the material and geometric properties as:

$E_1^f = 30.08 \cdot 10^9$ Pa, $E_2^f = 6.78 \cdot 10^9$ Pa,
$E^m = 3.45 \cdot 10^9$ Pa, $G_{12} = 3.01 \cdot 10^9$ Pa,
$v_f = 0.256$, $v_m = 0.3$,
$\rho_f = 1745$ kg/m^3, $\rho_m = 1200$ kg/m^3,
$l = 0.3$ m, $b = 0.03$ m,
$h = 0.00315$m, $\rho_{cnt} = 1300$ kg/m^3,
$v_{cnt} = 0.05$, $L_{cnt}/D_{cnt} = 50$,
$E_{cnt} = 1200 \cdot 10^9$ Pa, $\alpha = 0.00266°$.

3.1. Effect on CNT volume fraction on natural frequencies

The effect of CNT volume fraction on natural frequencies of a uniform and tapered composite beam is investigated by performing the simulation under various boundary conditions (including C-F, S-S and C-C) and different volume fraction of CNT. Simulation is performed by considering the stacking sequence of a uniform beam as $[0°/90°]_{8s}$ and a tapered beam $[0°/90°]_{8s}$ and $[0°/90°]_{4s}$ at thick and thin sections, respectively. The results are presented in Table 4. It can be seen that at all the modes considered, the natural frequencies increases with increasing the percentage

Table 4. Effect of CNT volume fraction [%] on natural frequencies [Hz] of CNT reinforced uniform and tapered composite beams under C-F, S-S and C-C end conditions.

End conditions	Composite beam configuration	Mode No.	CNT Volume fraction		
			$c_{cnt} = 0$	$v_{cnt} = 0.01$	$v_{cnt} = 0.05$
C-F end conditions	CNT reinforced uniform composite beam	1	19.89	30.34	55.05
		2	124.64	190.12	344.99
		3	349.00	532.34	965.99
		4	683.90	1043.20	1893.00
		5	1130.50	1724.50	3129.20
	CNT reinforced tapered composite beam	1	27.54	38.57	67.98
		2	134.41	187.97	330.41
		3	350.21	489.19	858.74
		4	667.91	932.55	1636.50
		5	1129.90	1578.90	2772.10
S-S end conditions	CNT reinforced uniform composite beam	1	55.83	85.16	154.53
		2	223.31	340.63	618.11
		3	502.46	766.42	1390.80
		4	893.26	1362.50	2472.50
		5	1395.70	2129.00	3863.20
	CNT reinforced tapered composite beam	1	54.39	75.97	133.32
		2	220.99	308.58	541.50
		3	495.57	692.11	1214.80
		4	900.58	1258.60	2210.00
		5	1380.20	1927.70	3383.40
C-C end conditions	CNT reinforced uniform composite beam	1	126.56	193.04	350.30
		2	348.86	532.13	965.61
		3	683.90	1043.20	1893.00
		4	1130.50	1724.50	3129.20
		5	1688.80	2576.10	4674.50
	CNT reinforced tapered composite beam	1	126.33	176.57	310.02
		2	347.05	484.77	850.84
		3	671.12	937.10	1644.50
		4	1136.80	1588.60	2789.10
		5	1680.10	2347.10	4120.20

content of CNT in composite beam. This is due to the fact that addition of CNT in composite beam enhances the specific stiffness of the composite beam which consequently increases the natural frequencies of the structure.

It can be also noticed that for the first mode at CF condition, first three natural frequencies of a tapered composite beam are much higher than those of with uniform composite beam, irrespective of the percentage volume fraction of CNT. For 1% CNT, the natural frequency of tapered composite beam found to be a little more than that of uniform composite beam at some initial modes of vibrations and CF conditions only. This is due to the right end of the beams are free. The reduction in the stiffness of the tapered composite beam is much lower than those in uniform composite beam which yields the higher natural frequencies. However, similar variation could not be seen in higher modes.

It is also shown that the natural frequencies of tapered composite beam are lower than those of with uniform beam under S-S and C-C end conditions. This can be allied to the ply orientation $[0°/90°]_{8s}$ and $[0°/90°]_{4s}$ at the right end of the uniform and tapered composite beams with simply supported end conditions. The enhancement in the stiffness of the tapered composite beam is much lower compared to uniform composite beam which yields the lower natural frequencies.

Similarly, it is realised that the natural frequencies of uniform and tapered composite beam with C-C end conditions are higher than other two boundary condi-

Table 5. Effect of aspect ratio of CNT on natural frequencies [Hz] of CNT reinforced uniform and tapered composite beams under C-F, S-S and C-C end conditions.

End conditions	Composite beam configuration	Mode No.	Aspect ratio of CNT		
			L_{CNT}/D_{CNT} = 0	L_{CNT}/D_{CNT} = 10	L_{CNT}/D_{CNT} = 50
C-F end conditions	CNT reinforced uniform composite beam	1	19.89	25.56	30.34
		2	124.64	160.16	190.12
		3	349.00	448.46	532.34
		4	683.90	878.81	1043.20
		5	1130.50	1452.70	1724.50
	CNT reinforced tapered composite beam	1	27.54	34.38	38.57
		2	134.41	167.80	187.97
		3	350.21	437.11	489.19
		4	667.91	833.53	932.55
		5	1129.90	1410.50	1578.90
S-S end conditions	CNT reinforced uniform composite beam	1	59.84	71.74	85.16
		2	239.35	286.96	340.63
		3	538.55	645.66	766.42
		4	957.42	1147.80	1362.50
		5	1496.00	1793.50	2129.00
	CNT reinforced tapered composite beam	1	54.39	67.89	75.97
		2	220.99	275.80	308.58
		3	495.57	618.50	692.11
		4	900.58	1124.20	1258.60
		5	1380.20	1722.60	1927.70
C-C end conditions	CNT reinforced uniform composite beam	1	126.56	162.63	193.04
		2	348.86	448.29	532.13
		3	683.90	878.82	1043.20
		4	1130.50	1452.70	1724.50
		5	1688.80	2170.20	2576.10
	CNT reinforced tapered composite beam	1	126.33	157.71	176.57
		2	347.05	433.18	484.77
		3	671.12	837.56	937.10
		4	1136.80	1419.10	1588.60
		5	1680.10	2097.00	2347.10

tions and with S-S is found to be more than that of with C-F end conditions. This fact is owing to C-C and C-F end conditions which yield the highest and the lowest stiffness and subsequently highest and lowest natural frequencies. Exclusively, average increase in natural frequency of tapered composite beam is considerably higher than the uniform composite beam at all boundary conditions and also increased in line with increase in % CNT reinforcement. This is by reason of uniform reduction of stiffness over the length of tapered composite beam compared to uniform composite beam.

3.2. Effect of aspect ratio on natural frequencies

The effect of aspect ratio (L_{CNT}/D_{CNT}) of CNT on natural frequencies of a uniform and tapered composite beam is investigated by performing the simulation under different boundary conditions (including C-F, S-S and C-C) and diverse aspect ratios of CNT. Simulation is performed by considering the stacking sequence of a uniform beam as $[0°/90°]_{8s}$ and a tapered beam $[0°/90°]_{8s}$ and $[0°/90°]_{4s}$ at thick and thin sections, respectively. The results are presented in Table 5. An enrichment in the natural frequencies can be noticed at all considered modes with increase in the aspect ratio of CNT in composite beam. This can also be related to the increase in stiffness of the structure with increase in aspect ratio of CNTs.

3.3. Effect of ply orientation on natural frequencies

The effect of ply orientation on natural frequencies of a uniform and tapered composite beam is in-

Table 6. Effect of aspect ratio of CNT on natural frequencies [Hz] of CNT reinforced uniform and tapered composite beams under C-F, S-S and C-C end conditions.

End conditions	Composite beam configuration	Mode No.	Different ply orientations		
			$[0°/30°]_{8s}$	$[0°/45°]_{8s}$	$[0°/90°]_{8s}$
C-F end conditions	CNT reinforced uniform composite beam	1	32.57	30.83	30.34
		2	204.11	193.22	190.12
		3	571.51	541.02	532.34
		4	1119.90	1060.20	1043.20
		5	1851.30	1752.60	1724.50
	CNT reinforced tapered composite beam	1	41.83	39.90	38.57
		2	203.05	194.12	187.97
		3	527.18	504.68	489.19
		4	1004.10	961.72	932.55
		5	1702.60	1629.30	1578.90
S-S end conditions	CNT reinforced uniform composite beam	1	91.42	86.55	85.16
		2	365.69	346.18	340.63
		3	822.81	778.91	766.42
		4	1462.80	1384.70	1362.50
		5	2285.60	2163.70	2129.00
	CNT reinforced tapered composite beam	1	81.86	78.37	75.97
		2	332.31	318.25	308.58
		3	745.59	713.90	692.11
		4	1357.50	1298.90	1258.60
		5	2076.80	1988.50	1927.70
C-C end conditions	CNT reinforced uniform composite beam	1	207.25	196.19	193.04
		2	571.28	540.81	532.13
		3	1119.90	1060.20	1043.20
		4	1851.30	1752.60	1724.50
		5	2765.60	2618.00	2576.10
	CNT reinforced tapered composite beam	1	190.45	182.22	176.57
		2	522.36	500.10	484.77
		3	1009.20	966.46	937.10
		4	1713.10	1639.30	1588.60
		5	2529.70	2421.50	2347.10

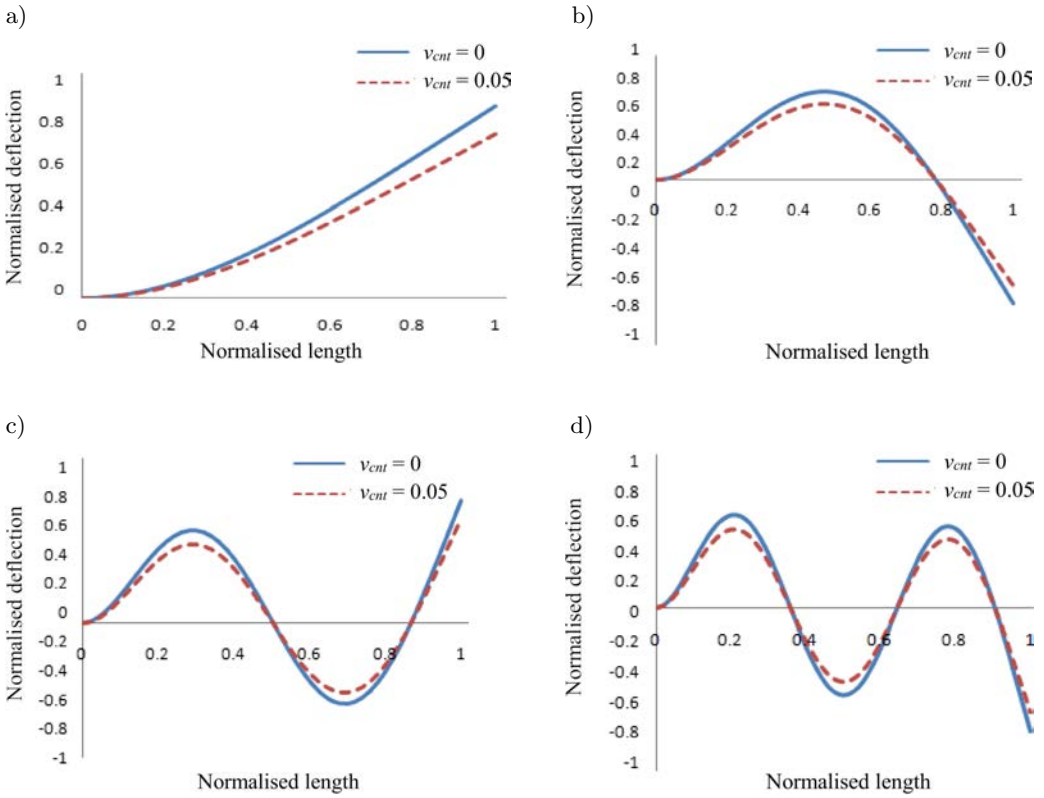

Fig. 3. Effect of CNT volume fraction on the first four mode shapes of a CNT reinforced uniform composite beam under C-F end condition: a) 1st mode shape, b) 2nd mode shape, c) 3rd mode shape, d) 4th mode shape.

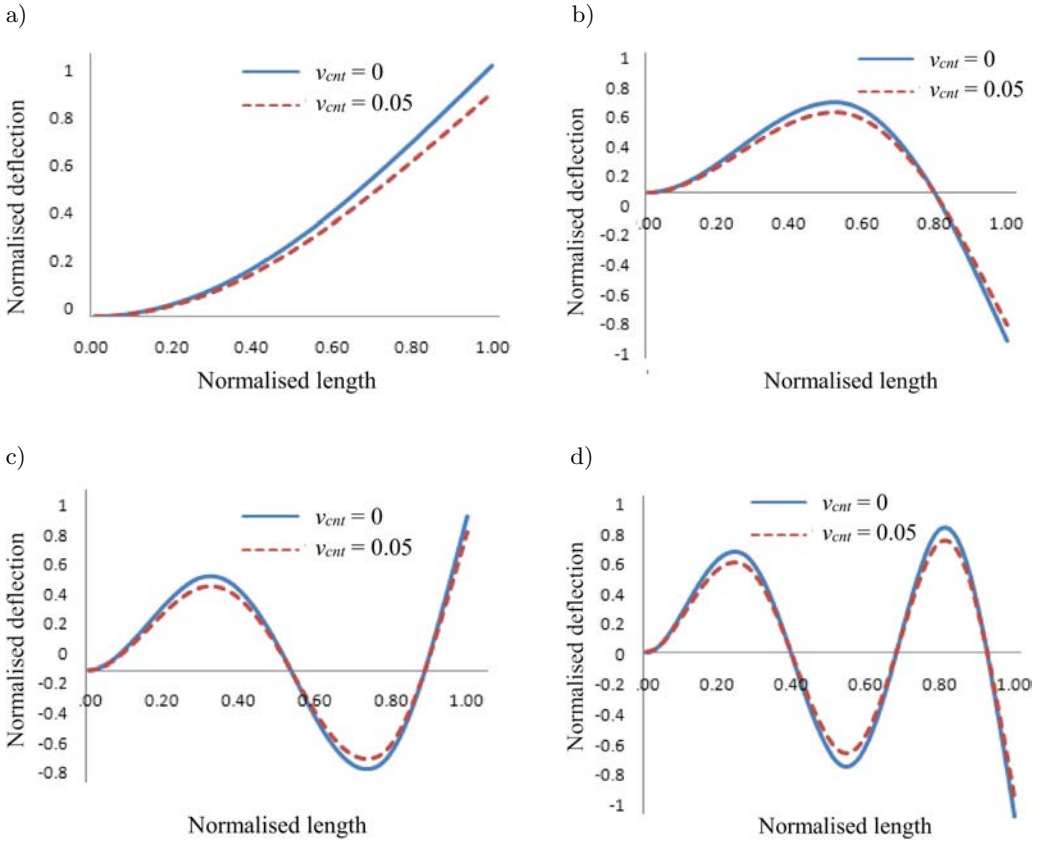

Fig. 4. Effect of CNT volume fraction on the first four mode shapes of a CNT reinforced tapered composite beam under C-F end condition: a) 1st mode shape, b) 2nd mode shape, c) 3rd mode shape, d) 4th mode shape.

vestigated by performing the simulation under several boundary conditions (including C-F, S-S and C-C) and different ply orientations. Simulation is performed by considering the different stacking sequences of uniform and tapered beams with CNT content and aspect ratios as 1% and 50, respectively. The results are presented in Table 6. The $[0°/30°]_{8s}$ yields the highest natural frequencies among the ply orientations considered.

3.4. Effect of CNT volume fraction on mode shapes

The effects of CNT volume fraction on free transverse vibration mode shapes of a uniform and tapered composite beam is investigated by performing the simulation under C-F end conditions. Simulation is performed by considering the stacking sequence of a uniform beam as $[0°/90°]_{8s}$ and a tapered beam $[0°/90°]_{8s}$ and $[0°/90°]_{4s}$ at thick and thin sections, respectively. The variation of the first four mode shapes with CNT content is presented in Figs 3 and 4, respectively for uniform and tapered composite beams. Substantial variation in the transverse vibration modes shapes is observed with increase in the percentage content of CNT. This shows the efficacy of CNT reinforcement in the FRP composite beams to enhance the level of stiffness of composite beams.

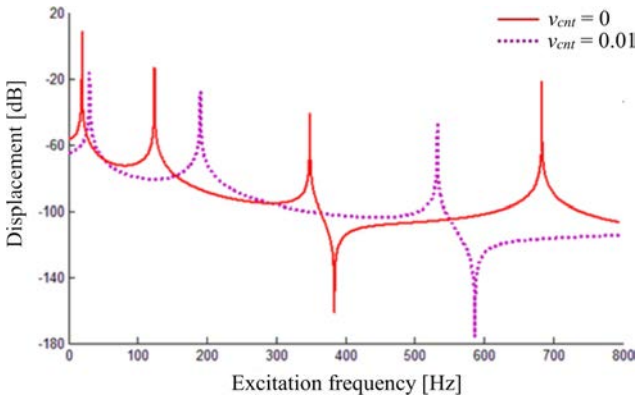

Fig. 5. Transverse vibration response of a CNT reinforced uniform composite beam under C-F end condition.

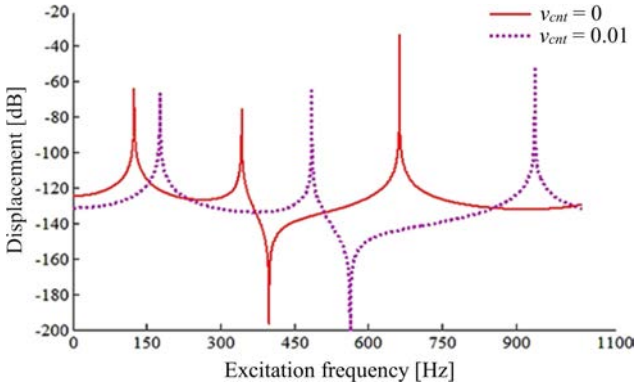

Fig. 6. Transverse vibration response of a CNT reinforced tapered composite beam under C-C end conditions.

3.5. Effect of CNT volume fraction on the transverse vibration of response

The effect of CNT volume fraction on the transverse vibration response of a CNT reinforced composite beams under C-F and C-C end conditions is investigated by considering magnitude of 1N applied at the centre of the beam. The responses of the beams are evaluated over the frequency range of 1–800 Hz under C-F end conditions for uniform composite beam and frequency range of 1–1100 Hz under C-C end condition for tapered composite beam where the CNT volume fractions are 0 and 0.01. Figures 5 and 6 show that the natural frequencies increase with increase in CNT volume fraction. It can be also witnessed that the magnitude of the peak response for all the modes decreases with increasing CNT volume fraction. This is once more evidence for the effectiveness of reinforcement of CNT into composite structures.

4. Conclusions

In this study, free vibration responses of uniform and tapered composite beams reinforced with carbon nanotubes are investigated. The governing differential equations of motion of a carbon nanotube (CNT) reinforced both uniform and tapered composite beams are presented in finite element formulation. The validity of the developed formulation is demonstrated by comparing the natural frequencies evaluated using present FEM with those of available in literature. The natural frequencies of a composite beam with and without CNT reinforcement are also compared. Results shows that the addition of CNT in fiber reinforced polymer composite beam enhance the natural frequencies considerably. Also, an increase in aspect ratio of CNT in composite beams significantly increases the natural frequencies. It is also shown that among $[0°/30°]_{8s}$, $[0°/45°]_{8s}$ and $[0°/90°]_{8s}$ laminates, the laminate with ply orientations $[0°/30°]_{8s}$ yield the highest natural frequencies. The transverse vibration mode shapes can be extensively altered by changing CNT content in composite beams. The forced vibration responses reveal the usefulness of CNT reinforcement in composite structures to reduce the peak deflection effectively. The results prove that CNT could be reinforced in fiber reinforcement polymer composite beam to tailor the free vibration characteristics of the composite beams.

Acknowledgments

Authors are grateful to Science and Engineering Research Board (SERB), Department of Science and Technology, Government of India, for providing financial support through the project entitled “A study of Structural damping and forced vibration responses of carbon nanotube Reinforced rotating Tapered Hybrid

composite plates" under the Grant No. SR/FTP/ETA-0009/2014 to carry out this work.

References

1. Andrews R., Wiesenberger M.C. (2004), *Carbon nanotube polymer composites*, Current Opinion in Solid State and Materials Science, **1**, 31–37.
2. Bakshi S.R., Batista R.G., Agarwal A. (2009), *Quantification of carbon nanotube distribution and property correlation in nanocomposites*, Composites: Part A, **40**, 1311–1318.
3. Cleghorn W.L., Tabarrok B. (1997), *Finite element formulation of a tapered Timoshenko beam for free vibration analysis*, Journal of Sound and Vibration, **152**, 3, 461–470.
4. Dai R.L., Liao W.H. (2009), *Fabrication, testing, and modelling of carbon nanotube composites for vibration damping*, Journal of Vibration and Acoustic, **131**, 1–9.
5. de Borbon F., Ambrosini D., Curadelli O. (2014), *Damping response of composites beams with carbon nanotubes*, Composites: Part B, **60**, 106–110.
6. Deepak B.P., Ganguli R., Gopalakrishnan S. (2012), *Dynamics of rotating composite beams: A comparative study between CNT reinforced polymer composite beams and laminated composite beams using spectral finite elements*, International Journal of Mechanical Sciences, **64**, 110–126.
7. El-Maksoud Abd M.A. (2000), *Dynamic analysis and buckling of variable thickness laminated composite beams using conventional and advanced finite element formulations*, Master of applied Science Thesis, Department of Mechanical Engineering, Concordia University.
8. Fidelus J.D., Wiesel E., Gojny F.H., Schulte K., Wagner H.D. (2005), *Thermo-mechanical properties of randomly oriented carbon/epoxy nanocomposites*, Composites Part A: Applied Science and Manufacturing, **36**, 1555–1561.
9. Gibson R.F., Ayorinde E.O., Wen Y.F. (2007), *Vibrations of carbon nanotubes and their composites: a review*, Compos Science and Technology, **67**, 1–28.
10. He K., Hoa S.V., Ganesan R. (2000), *The study of tapered laminated composite structures: a review*, Composites Science and Technology, **60**, 2643–2657.
11. Iijima S. (1999), *Helical microtubules of graphitic carbon*, Nature, **8**, 354–356.
12. Jakkamputi L.P., Rajamohan V. (2017), *Dynamic characterization of CNT-reinforced hybrid polymer composite beam under elevated temperature – an experimental study*, Polymer Composites, doi: 10.1002/pc.24668.
13. Khan S.U., Li C.Y., Siddiqui N.A., Kim J.-K. (2011), *Vibration damping characteristics of carbon fiber-reinforced composites containing multi-walled carbon nanotubes*, Composites Science and Technology, **71**, 1486–1494.
14. Ko F.K. (2004), *Nanofiber Technology: Bridging the Gap Between Nano and Macro World*, [in:] *Nanoengineered Nanofibrous Materials*, Guceri S., Gogotsi Y.G., Kuznetsov V. [Eds.], pp. 1–18, Kluwer Academic Publishers, Dordrecht.
15. Lin R.M., Lu C. (2010), *Modelling of interfacial friction damping of carbon nanotube based nanocomposites*, Mechanical Systems and Signal Processing, **24**, 2996–3012.
16. Moser K., Lumassegger M. (1988), *Increasing the damping of flexural vibration of laminated FPC structures by incorporation of soft intermediate plies with minimum reduction of stiffness*, Composite Structures, **10**, 321–333.
17. Qu Y., Long X., Li H., Meng G. (2013), *A variational formulation for dynamic analysis of composite laminated beams based on a general higher-order shear deformation theory*, Composite. Structures, **102**, 175–192.
18. Ramaratnam A., Jalili N. (2006), *Reinforcement of piezoelectric polymers with carbon nanotubes: pathway to next-generation sensors*, Journal of Intelligent Material Systems and Structures, **17**, 199–208.
19. Rao S.S. (2011), *Mechanical Vibration*, 5th Ed., Pearson Education, University of Miami.
20. Ruoff R.S., Qian D., Liu W.K. (2003), *Mechanical properties of carbon nanotubes: theoretical predictions and experimental measurements*, Comptes Rendus Physique, **4**, 9, 993–1008.
21. Saravanos D.A., Pereira J.M. (1992), *Effects of interply damping layers on the dynamic characteristics of composite plates*, American Institute of Aeronautics and Astronautics, **30**, 12, 2906–2913.
22. Savvas D.N., Papadopoulos V., Papadrakakis M. (2012), *The effect of interfacial shear strength on damping behaviour of CNT reinforced composites*, International Journal of Solids and Structures, **49**, 3823–3837.
23. Shi D., Feng X., Huang Y.Y., Hwang K., Gao H. (2004), *The effect of nanotube waviness and agglomeration on the elastic property of carbon nanotube-reinforced composites*, Journal of Engineering Materials and Technology, **126**, 250–257.
24. Soutis C. (2005), *Carbon fiber reinforced plastics in aircraft construction*, Material Science Engineering, **412**, 1, 171–176.
25. Tan H., Jiang L.Y., Huang Y., Liu B., Hwang K.C. (2007), *The effect of van der Waals-based interface cohesive law on carbon nanotube-reinforced composite materials*, Composite Science and Technology, **67**, 2941–2946.
26. Thomas J., Abbas A.H. (1978), *Finite element model for dynamic analysis of Timoshenko beams*, Journal of Sound and Vibration, **60**, 11–20.
27. Thostenson E.T., Chou T.W. (2002), *Aligned multi-walled carbon nanotube reinforced composites: processing and mechanical characterization*, Journal of Physics D: Applied Physics, **35**, 77–80.
28. Zabihollah A., Ganesan R. (2007), *Vibration analysis of tapered composite beams using a higher-order finite element. Part II: parametric study*, Composite Structures, **77**, 306–318.